

Supplement of Biogeosciences Discuss., 11, 12341–12373, 2014
<http://www.biogeosciences-discuss.net/11/12341/2014/>
doi:10.5194/bgd-11-12341-2014-supplement
© Author(s) 2014. CC Attribution 3.0 License.



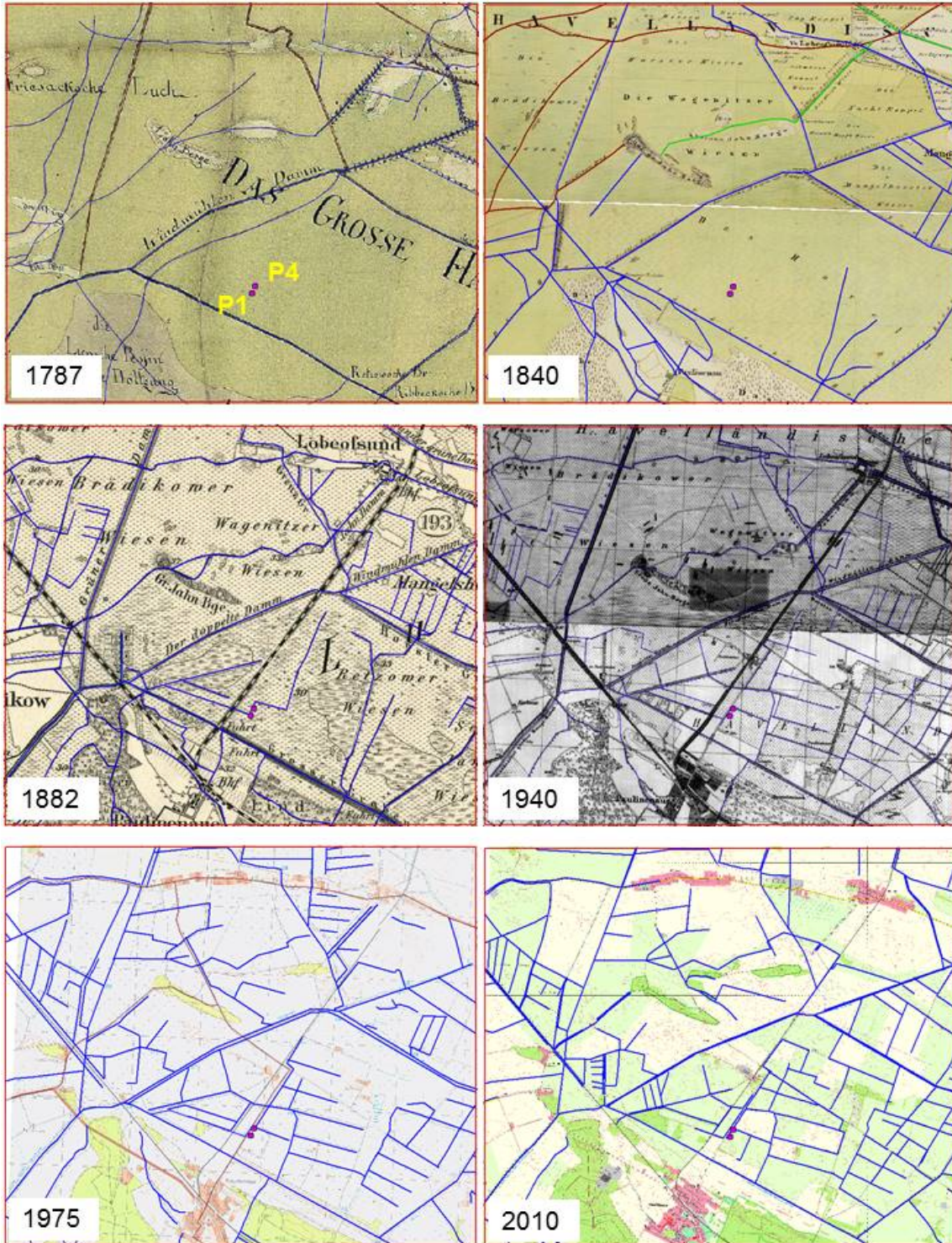
Supplement of

Are C-loss rates from drained peatlands constant over time? The additive value of soil profile based and flux budget approach

J. Leifeld et al.

Correspondence to: J. Leifeld (jens.leifeld@agroscope.admin.ch)

20 Figure S1: Land use and ditches (in blue) in the “Havelländische Luch” near Paulinenaue from 1787 to
 21 2010; rectangles: 7km x 6km = 42 km²; sources: Schmettau Map (1787); Prussian Land Survey Maps
 22 (1840, 1882), Topographic Map of Deutsches Reich (1940); Modern Topographic Maps (1975, 2010);
 23 original map scales = 1:25,000 (except Schmettau Map); for details, please contact: sommer@zalf.de



24

25

26 Table S1: Annual carbon balance, groundwater level, and precipitation for the 5y observation period;
27 number in brackets = standard deviation

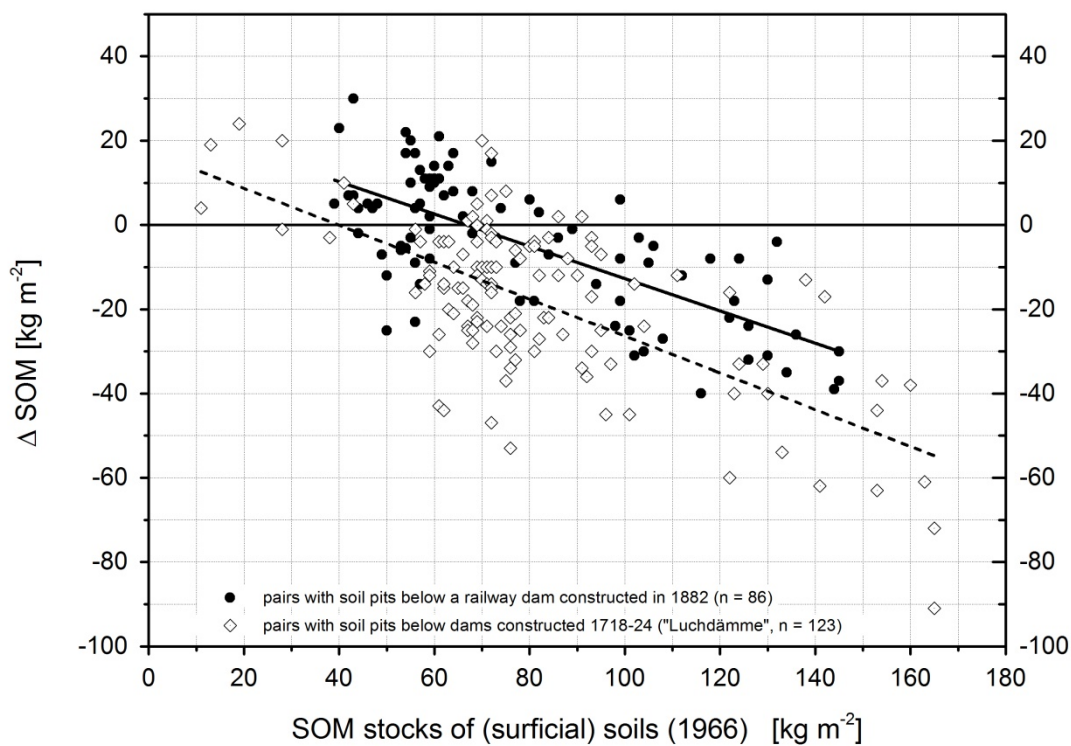
28

Year	C-balance (g C m⁻² a⁻¹)		Groundwater Level (m)		Precipitation (mm)
Site	P1	P4	P1	P4	
2007-2008	513 (35)	98 (51)	-0.11 (0.19)	-0.05 (0.19)	1011
2008-2009	770 (36)	877 (66)	-0.42 (0.18)	-0.38 (0.16)	454
2009-2010	545 (24)	856 (37)	-0.41 (0.27)	-0.36 (0.23)	512
2010-2011	1010 (56)	1946 (50)	-0.26 (0.24)	-0.24 (0.23)	564
2011-2012	717 (29)	753 (63)	-0.22 (0.24)	-0.20 (0.22)	658
5y-mean	711	906	-0.28	-0.23	640
5y-sd	200	664	0.23	0.21	221

29

30

31 Figure S2: Influence of SOM stocks (surficial soils, 1966) on SOM changes [Δ SOM] over time, with Δ SOM
32 = SOM stocks of surficial soils (1966) minus adjacent buried soils under dams, ie "Luchdämme" (1718-
33 24) and railway dam Paulinenaue-Neuruppin (1882); negative values = SOM losses, positive values =
34 SOM gains for period 1882-1966 (railway dam) or 1720-1966 ("Luchdämme"); data source: Gerhart
35 Mundel: Studies on the genesis of the "Havelländisches Luch" and its changes related to amelioration in
36 due consideration of peat mineralization (in German). PhD thesis, German Academy of Agricultural
37 Sciences, Berlin, 1969.



38

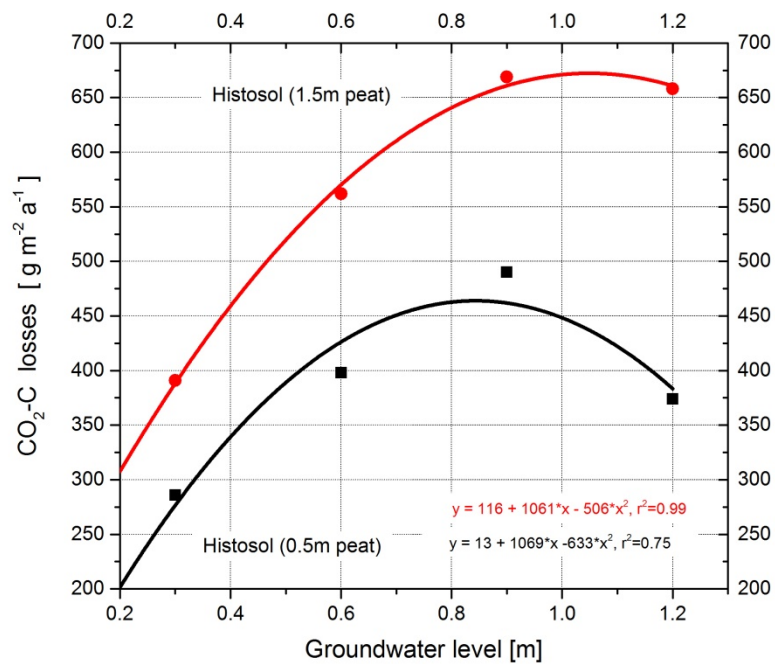
39

40

41

42 Figure S3: Lysimeter experiments on the influence of groundwater level on CO₂ losses from two Histosols
43 under grassland; mean annual CO₂ losses during 1968-1970 (3y); data source: G. Mundel. Studies on
44 peat mineralization in fens (in German). Arch.Acker-u.Pflanzenbau u. Bodenkd. 10, 669-679, 1976.

45



46

47

48 **Supplement to Material and Methods**

49 **1.1 Gas flux measurements**

50 Biweekly measurements of CH₄ emissions were conducted by a static closed (Non-Flow-Through Non-
51 Steady-State (NFT-NSS)) chamber system (Livingston and Hutchinson 1995), whereas measurements of
52 CO₂-exchange were compiled all three to four weeks, using a dynamic closed (Flow-Through Non-Steady-
53 State (FT-NSS)) chamber system (Drösler 2005).

54 The dynamic system consists of a portable infrared gas analyzer (LI 820 gas analyzer [LI-COR Biosciences,
55 Lincoln, Nebraska, USA]) and manually operated, cubic opaque and transparent PVC chambers with a
56 light transmission of 76%. The chambers sized 0.56 m² at the base and had a total volume of 0.296 m³.
57 To avoid biased air stratification, the chambers were equipped with two adjustable fans, assure efficient
58 headspace mixing during measurements. Transparent and non-transparent extensions (0.296 m²) as well
59 as external fans were used to enlarge the chamber volume appropriate to plant height and minimize
60 plant irritation (Li et.al. 2008). Airtight closure was ensured by rubber foam cartridge seals at the bottom
61 of the chambers. Identical sized opaque PVC chambers, equipped with four vents for taking gas samples
62 were used for CH₄ measurements. Within the deployment time of 60 minutes, four samples are drawn at
63 20 minutes intervals by the placement of vacuumed glass vials on the vents. Taken gas samples were
64 analyzed for CO₂-, CH₄- and N₂O-concentrations using a gas chromatograph, equipped with flame
65 ionization detector (FID) and electron capture detector (ECD) (Shimadzu 14A). To estimate R_{eco}- (opaque)
66 and NEE-fluxes (transparent), chambers were deployed on the three repetitive plots of the measurement
67 site, marked by cubic PVC collars. The CO₂-concentration in ppm inside the chambers was determined at
68 5 second intervals during separated, five minute measurements. To cover a broad variance of air and soil
69 temperatures (opaque chambers) and photosynthetic active radiation (PAR) (transparent chambers),
70 continuously measurements were conducted over the course of one to two bright days, starting before
71 sunrise. In order to relate the CO₂ fluxes to prevailing environmental conditions, the photosynthetic
72 photon flux density, the air temperature inside and outside the chamber, soil temperatures in 2, 5 and
73 10 cm depth (respectively water temperature), as well as the water level was currently recorded during
74 measurements (Alm et. al. 2007). Measurement campaigns were realized once a month in growing
75 season and fall, to once all six weeks during wintertime (Li et.al. 2008).

76

77 **1.1.1 FLUX calculation**

78 Gas fluxes were calculated under consideration of chamber volume, basal area, air temperature and air
79 pressure according to the ideal gas law using linear regression. CH₄ fluxes were computed, using the R

80 package FLUX. The evolution of the CO₂ concentration in the chamber headspace over time was,
81 however, analyzed by a variable moving window approach and certain flux calculation algorithm
82 (Hoffmann et. al 2014). Thereby ,5% of data points were discarded at both ends of a measurement, to
83 avoid noise in the data, due to turbulences and pressure disturbances, as well as ascending saturation
84 and canopy microclimate effects caused by initial chamber deployment (Kutzbach et. al. 2007,
85 Langensiepen et.al. 2012).

86

87 1.1.2 Parameter estimation

88 R_{eco}-model parameters were compiled for each CO₂-flux-set by using the temperature dependent
89 Arrhenius-type R_{eco}-flux model of Lloyd and Taylor (1994).

90

$$R_{eco} = R_{ref} * e^{E_0 \left(\frac{1}{T_{ref}-T_0} - \frac{1}{T-T_0} \right)}$$

91

92 With R_{eco} the measured ecosystem respiration rate [$\mu\text{mol}^{-1} \text{m}^{-2} \text{s}^{-1}$], R_{ref} the respiration at reference
93 temperature (T_{ref}) [283.15 K], T₀ the temperature constant for the beginning of biological processes
94 [227.13 k] and T as the mean temperature over the turn of the flux measurement in 2 cm, 5 cm and 10
95 cm soil depth or air temperature in 20 cm height, respectively.

96 The lowest Akaike Information Criterion (AIC) was chosen to compute GPP-fluxes by model and subtract
97 R_{eco} of NEE measurements. In case Lloyd and Taylor equation was not applicable to the data-set, the
98 average of measured non-transparent CO₂-fluxes was used.

99 PAR dependent GPP-flux models for each CO₂-flux-set were calculated according to the rectangular,
100 hyperbolic light response equation of Michaels and Menten (1913).

101

$$GPP = \frac{GP_{max} * \alpha * PAR}{\alpha * PAR + GP_{max}}$$

102

103 With GPP the calculated gross primary productivity [$\mu\text{mol}^{-1} \text{m}^{-2} \text{s}^{-1}$], GP_{max} the maximum rate of carbon
104 fixation at infinite PAR [$\text{CO}_2\text{-C mg m}^{-2} \text{h}^{-1}$], α the light use efficiency [$\text{CO}_2\text{-C mg m}^{-2} \text{h}^{-1}$] and PAR the
105 photon flux density of the photosynthetic active radiation [$\mu\text{mol}^{-1} \text{m}^{-2} \text{s}^{-1}$].

106 Due to chamber induced light transmission loss, PAR was corrected by -14% before applying to eq. (2).

107 GPP-parameters with lowest AIC were used for modeling process. In case the parameter estimation for
108 eq. (2) was not possible or insignificant a nonrectangular hyperbolic light-response function was used
109 (Glimanow et. al. 2013). This usually resulted in significant estimates of parameters.

110

$$GPP = \alpha * PAR + GP_{max} - \sqrt{(\alpha * PAR + GP_{max})^2 - 4 * \alpha * PAR * GP_{max} * \theta}$$

111

112 With θ the convexity coefficient of the light-response equation (dimensionless).

113 However, if no negative correlation between data-sets and PAR was found, an average parameters
114 approach was used. Under the general assumption of declining GPP-fluxes between 0 and 100 $\mu\text{mol}^{-1} \text{m}^{-2}$
115 s^{-1} the parameters α and GP_{max} were set on -0.01 and the average of measured GPP-fluxes, respectively.

116

117 **1.1.3 Modelling approach**

118 Annual CH_4 emissions were calculated by simple linear interpolation between campaigns. To model R_{eco} ,
119 GPP and NEE, the records of prevailing environmental conditions and determined parameters of R_{eco} and
120 GPP were used. Before applying these parameters on the environmental controls temperature and PAR,
121 measured air and soil temperatures were corrected. Paired difference tests were performed to obtain
122 spatial heterogeneity within the temperature values. Subsequently, site related climate data was
123 generated by correlating records of the climate station with temperature values obtained during the gas
124 exchange measurement. To gain the final NEE-model, Parameter estimates of R_{eco} and GPP were applied
125 to recalculated best-fit temperatures and PAR, respectively. Thereby computed fluxes of R_{eco} and GPP
126 were blended between campaigns, using a weighted average. To avoid influence of the previous and
127 following campaign parameters on flux estimates of the day of measurement, determined parameters
128 were maintained stable between the first and last measurement of a campaign. Finally NEE was
129 calculated as the sum of R_{eco} and GPP.

130

131 **1.1.4 Error prediction**

132 Besides the error of calculated fluxes and measured temperatures and PAR, mayor uncertainty arises
133 from site specific temperature models as well as parameter estimation for R_{eco} and GPP. Furthermore,
134 temporal interpolation of modeled fluxes between measurement campaigns is of crucial importance.
135 Moreover, significant uncertainty may also occur due to irreducible random variability (Moriasi et al.
136 2007). To include mentioned sources of error, uncertainty quantification of modeled R_{eco} , GPP and NEE
137 fluxes was performed by a comprehensive error prediction as following:

- 138 (i) In order to address the occasionally small samples size of below $n=30$, bootstrap
139 confidence intervals were used to calculate the error of measured CO_2 -fluxes
140 (ii) Consecutively, confidence intervals for estimated parameter sets of R_{eco} , GPP and the
141 temperature model were determined ($\alpha=0.01$). In case parameter estimation
142 failed the standard deviation was used to compute the confidence interval of the
143 given average flux or temperature value
144 (iii) Afterwards, 1000 different temperature models were created, by randomly sampling
145 each temperature value within the calculated confidence range. Similarly, parameter
146 sets for R_{eco} and GPP were 1000 times randomly sampled as well, using case
147 resampling
148 (iv) Maintained parameter sets and temperature models were subsequently used to
149 compute R_{eco} and GPP models between two campaigns
150 (v) Accordingly, resulted campaign interspace specific sums of R_{eco} and GPP-fluxes were
151 bootstrapped and the 0.01 and 0.99 quantile was calculated
152 (vi) Finally, the total uncertainty for modeled NEE and given probability was estimated,
153 following the law of error propagation

154 The same algorithm was applied to estimate the model error of interpolated CH_4 emissions, by using the
155 campaign specific average CH_4 fluxes and linear interpolation between campaign values.

156
157 **References**
158 Alm, J., Shurpali, N.J., Tuittila, E-S., Laurila, T., Maljanen, M., Saarnio, S., Minkkinen, K. Methods for
159 determining emission factors for the use of peat and peatlands – flux measurements and
160 modelling. *Boreal Environment Research*, 12, pp. 85-100, 2008
161 Drösler, M. Trace gas exchange of bog ecosystems, Southern Germany, PhD thesis, Technische
162 Universität München, Munich, 179pp., 2005.
163 Gilmanov, T.G., Wylie, B.K., Tieszen, L.L., Meyers, T.P., Baron, V.S., Bernacchi, C.J., Billesbach, D.P.,
164 Burba, G.C., Fischer, M.L., Glenn, A.J., Hanan, N.P., Hatfield, J.L., Heuer, M.W., Hollinger, S.E.,
165 Howard, D.M., Matamala, R., Prueger, J.H., Tenuta, M., Young, D.G.. CO_2 uptake and
166 ecophysiological parameters of the grain crops of midcontinent North America: Estimates from
167 flux tower measurements. *Agriculture, Ecosystems and Environment*, 164, 162–175, 2013.
168 Hoffmann, M., Jurisch, N., Borraz, E.A., Hagemann, U., Augustin, J., Drösler, M. Sommer, M. Auto-mated
169 modeling of ecosystem CO_2 fluxes based on periodic closed chamber measurements: A
170 standardized conceptual and practical approach. Submitted to *Agric. Forest Meteorol.* 2014.
171 Kutzbach, L., Schneider, J., Sachs, T., Giebels, M., Nykänen, H., Shurpali, N.J., Martikainen, P.J., Alm, J.,
172 Wilmling, M. CO_2 flux determination by closed-chamber methods can be seriously biased by
173 inappropriate application of linear regression. *Biogeosciences*, 4, 1005–1025, 2007.

174 Langensiepen, M., Kupisch, M., van Wijk, M. T., Ewert, F. Analyzing transient closed chamber effects on
175 canopy gas exchange for flux calculation timing. *Agric. Forest Meteorol*, 164, 61–70, 2012. Li,
176 Y.-L., Tenhunen, J., Owen, K., Schmitt, M., Bahn, M., Drösler, M., Otieno, D., Schmidt, M.,
177 Grünwald, T., Hussain, M.Z., Mirzae, H., Bernhofer, C. Patterns in CO₂ gas exchange capacity of
178 grassland ecosystems in the Alps. *Agric. Forest Meteorol*. 148, 51–68, 2008.

179 Livingston, G.P., Hutchinson, G.L. Enclosure-based measurement of trace gas exchange: Applications
180 and sources of error. In: P. A. Matson, R. C. Harris (Eds.), *Methods in Ecology. Biogenic Trace*
181 *Gases: Measuring Emissions From Soil and Water*. Blackwell Science, Malden, pp.14–51
182 (1995) Lloyd, J., Taylor, J.A. On the temperature dependence of soil respiration. *Funct. Ecol.* 8
183 315–323, 1994.

184 Michaelis, L., Menten, M.L. Die Kinetik der Invertinwirkung. *Biochem Z* 49, 333–369, 1913.

185 Moriasi, D. N., Arnold, J.G., Van Liew, M.M., Binger, R.L., Harmel, R.D., Veith, T. Model evaluation
186 guidelines for systematic quantification of accuracy in watershed simulations, *Transactions of the*
187 *ASABE*, 50, 885-900, 2007.

188